Volume 1 | Number 1 | Jan 2013 | Pages 1–100

Lab on a Chip

Miniaturisation for chemistry, physics, biology, materials science and bioengineering
www.rsc.org/loc

ROYAL SOCIETY OF CHEMISTRY

This is an *Accepted Manuscript*, which has been through the Royal Society of Chemistry peer review process and has been accepted for publication.

Accepted Manuscripts are published online shortly after acceptance, before technical editing, formatting and proof reading. Using this free service, authors can make their results available to the community, in citable form, before we publish the edited article. We will replace this *Accepted Manuscript* with the edited and formatted *Advance Article* as soon as it is available.

You can find more information about *Accepted Manuscripts* in the **Information for Authors**.

ARTICLE

Single chip SPR and fluorescent ELISA assay of prostate specific antigen

J. Breault-Turcot[a], H.-P. Poirier-Richard[a], M. Couture[a], D. Pelechacz[a] and J.-F. Masson[a,b]*

A multi-channel system combining fluidics and micropatterned plasmonic materials with wavelength interrogation surface plasmon resonance (SPR) and fluorescence detection was integrated from the combination of a small and motorized fluorescence microscope mounted on a portable 4-channel SPR instrument. The SPR and fluorescent measurements were performed based on the same detection area in a multi-channel fluidic, with a sensing scheme for prostate-specific antigen (PSA) consisting of a sandwich assay with a capture anti-PSA immobilized onto the SPR sensor and a detection anti-PSA modified with horseradish peroxidase (HRP). In this dual-detection instrument, fluorescence was measured from the solution side of the micropatterned gold film, while the interface between the glass prism and the gold film served to interrogate the SPR response. The SPR sensors were comprised of microhole arrays fabricated by photolithography to enhance the instrumental response for PSA detection by approximately a factor of 2 to 3 and they were coated with a self-assembled monolayer of a peptide (3-MPA-HHHDD-OH) to minimize nonspecific adsorption. PSA was successfully detected at clinical concentrations from 10 pM to 50 nM with this integrated system in a single assay lasting 12 minutes, almost centering on the desired range for PSA diagnostic tests (> 4 ng/mL or > 150 pM). The combination of two robust techniques in a single chip and instrument has led to a simple and effective assay that can be carried out on a small and portable instrument providing rapid biodetection of an important cancer biomarker with a dynamic range of nearly 4 orders of magnitude in the clinical range.

Introduction

ELISA is a common method of surface-based detection for a variety of analytes and is currently the workhorse of clinical laboratories. In an ELISA test, the analyte is captured on a surface modified with a bioreceptor and detection occurs through the use of secondary antibodies modified with an enzyme that reacts with a colorimetric or fluorescent molecule. While ELISA assays are robust, they suffer from long incubation times and several steps that lengthen the detection process. Surface plasmon resonance (SPR) sensing is an optical technique sensitive to biomolecules[1] and detection with SPR technologies can be achieved with specific receptors such as aptamers[2,3], antibodies[4] or antibody fragments[5]. The principles of SPR sensing are analogous to ELISA, where the bioreceptor is immobilized on the surface of the SPR sensor and the analyte captured. Unlike ELISA, SPR sensing is a label free technique providing real-time measurements of biomolecular interactions. Thus, SPR directly detects the binding event of an analyte on the sensor and does not require the conversion of the colorimetric or fluorescent reagent to quantify biomolecules. SPR sensing is also amenable to miniaturization of the instrumentation and rapid analysis SPR sensing has been extensively used for characterization and quantification of a variety of proteins with limits of detection in the low nanomolar to picomolar range [6-9].

The advances in microfluidic technologies led to the engineering of smaller devices providing faster response for point-of-care applications. ELISA assays were thus developed on lab-on-a-chip platforms for a variety of applications in the medical field [10-17]. Portable systems assembled from readily accessible instrumental components and detector such as a smartphone were recently integrated for an ELISA assay monitoring antibodies associated to different medical conditions[18]. In addition to the classical optical detection using fluorescence or UV-Vis, it is possible to integrate sensors in the microfluidic platform, such as electrochemical detection [19], surface enhanced Raman scattering [20] or surface plasmon resonance [21]. The integration of multiple detection modalities can provide a built-in positive control for monitoring a disease marker if the techniques are not susceptible to the same interferences. For example, SPR sensing is especially susceptible to nonspecific binding of background molecules to the sensor while fluorescence-ELISA is generally insensitive to the binding of interferents to the sensor, as the response is revealed with the specific interaction of the secondary antibody with the analyte and the enzymatic response of the

[a] Département de chimie, Université de Montréal, C.P. 6128 Succ. Centre-Ville, Montreal, Qc, Canada, H3C 3J7
[b] Centre for self-assembled chemical structures (CSACS)
*Contact information: Tel: +1-514-343-7342; Fax: +1-514-343-7586; jf.masson@umontreal.ca

Please do not adjust margins
Lab on a Chip
Page 2 of 8

secondary antibody. ELISA requires low background fluorescence and is susceptible to optical interferences from absorbing species. In SPR sensing, the light beam indirectly interacts with the sample and is relatively insensitive to optical interferences. The combination of techniques such as SPR and fluorescence ELISA in a single platform could provide a confirmatory measurement.

In many medical applications, the level of biomarkers can vary by several orders of magnitude in clinical samples. However, the linear dynamic range of ELISA and affinity sensors such as SPR is limited to around 2 orders of magnitude due to the thermodynamics of the Langmuir isotherm. Several strategies have been employed to extend the dynamic range of biosensors, including the modification of bioreceptors [22-25], the combination of several bioreceptors with different affinities on a single biosensor [26-28], enhancing the response obtained in the low concentration region of the Langmuir isotherm [29] and the use of a nanoplasmonic electrical field-enhanced sensor as the biosensing template [30]. The integration of multiple detection modalities in a single microfluidic platform can also provide the advantage of extended dynamic range if techniques have different but overlapping dynamic ranges, which is the case for SPR sensing and ELISA.

Several studies have compared the performance of SPR and ELISA [31-38]. SPR sensing was shown to be collinear with ELISA for the detection of anti-asparaginase [31]. In some cases, the sensitivity of SPR was similar to ELISA, such as for CD166/ALCAM [37] and for toxins [32]. In other cases, ELISA was more sensitive than SPR, which was demonstrated for albumin [38], human hepatitis B virus (HBV) [33] and for ricin [35]. The amplification of an SPR response with secondary antibodies increased the sensitivity of the SPR sensor and thus, narrowed the gap in sensitivity between ELISA and SPR sensing in other applications [33]. All these previous reports were based on dedicated SPR and ELISA instruments, and they have to the best of our knowledge never been combined in a single platform. Regardless, these comparative studies revealed that SPR and ELISA have different but nearly overlapping dynamic ranges, which may be suited to increase the overall dynamic range of an assay if SPR and ELISA are combined in a single instrument.

The concept of SPR-ELISA is demonstrated here for the detection of prostate specific antigen (PSA), a common cancer biomarker. This model protein is one of several biomarkers indicative of the presence or the stage of certain diseases such as myocardial infarction [39], congestive heart failure [40] or cancers [41,42]. PSA is secreted in the blood of patients with a healthy prostate at concentrations of around 0.01 to 0.1 nM for 50 years old men [43]. A concentration of PSA in blood above 0.15 nM (4 ng/mL) is considered high and is the common threshold to screen for prostate cancer. Prostate cancer is among the most prevalent cancers in western countries, especially in men over 50 years old. However, the number of deaths by prostate cancer has slowly started to decrease in

Canada since the 90's with the advent of extensive screening of men at risk and the screening of PSA levels in blood. Those two aspects have played a major role in the early diagnosis of prostate cancer and the increased survival rate. Screening of prostate cancer is generally performed by ELISA tests for PSA. These tests are still carried out in centralized laboratories and the turnaround time remains an important challenge in PSA screening. The detection of PSA in buffer solutions has been reported using SPR detection [44] and a sandwich assay [45] achieving detection limits of ng/mL for this biomarker. However, this analysis was performed on large and costly laboratory instruments. To address the challenges associated with ELISA in PSA testing, we report here on the use of a small and portable dual-detection system to perform PSA detection using both SPR and ELISA coupled with fluorescence detection.

Experimental details

The source of the materials and chemicals used is provided as supporting information. BK7 glass wafers of 4 inches in diameter and dove glass prism of 20 x 12 x 2.5 mm were all cleaned with warm piranha solution (sulphuric acid + hydrogen peroxide – 3 : 1 at approx. 80°C – *Caution! Piranha solution is highly corrosive*) for 20 and 90 minutes, respectively. All glass substrates were washed vigorously with deionised water to remove any traces of piranha solution and dried with a stream of nitrogen. Glass prisms were covered with a smooth and continuous gold film by directly sputtering 0.5 nm chromium and 45 nm gold (Cressington 308R sputter coater, Ted Pella Inc. Redding, CA). An argon pressure of 0.02 mbar and a current set at 80 mA were used during sputtering.

The microhole array substrates were fabricated with standard photolithography techniques. Cleaned BK7 glass 4" wafers were primed with HDMS for 90 seconds at 120°C (310TA oven, Yield Engineering Systems, Livermore, CA). Resins (LOR1A and OIR 674-11) were spin coated onto the primed-wafers according to the manufacturer's directives. The resins were exposed with a dose of 73.8 mW through a disk-patterned mask (Photomask portal, Richardson TX) using a MA6 mask aligner from SUSS MicroTec (Sunnyvale, CA). A post-exposure bake was then performed at 90°C for 90 seconds. The resins were then developed for 90 seconds in AZ726 MIF. Subsequently, 1 nm of chromium and 65 nm of gold were deposited on the wafers with ebeam lithography. Lift off of the photoresin mask was carried out in Remover PG in a sonic bath for 10 minutes. To fit on the dove prisms, the substrates were then cut into 11 X 17 mm chips with a 7100 Provectus dicing saw (Advanced Dicing Technology, Horsham, PA). Scanning electron microscopy (SEM, Jeol, Peabody, MA) and atomic force microscopy (AFM, WItec, Ulm, Germany) were used to validate the thickness of the metallic layer.
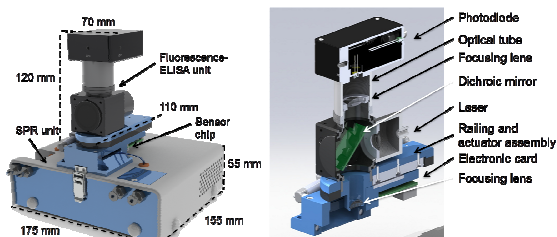
Microfluidic fabrication

Figure 1. (Left panel) Representation of the SPR-fluorescence-ELISA instrument. The sensor chip (not seen) was mounted at the interface between both units. (Right panel) Design of the fluorescence-ELISA unit for the SPR instrument. Standard components of an epifluorescence microscope were included in the unit (laser entry, lenses, optical tube, dichroic mirror, and a photodiode), in addition to the railing and actuator system for moving the fluorescence unit from channel to channel.
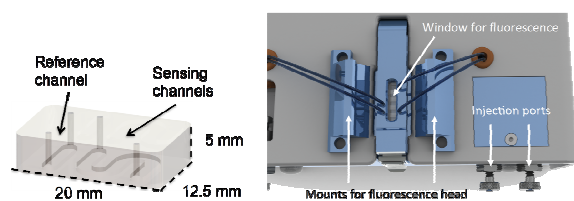

Figure 2. (Left panel) Schematic representation of the fluidic cell. The SPR sensor is located below the fluidic cell and the fluorescence unit was located above the fluidic cell. (Right panel) The modifications to the SPR instrument required carving an optical window in the latch arm and adding the mounts for the fluorescence head.

The PDMS fluidics were prepared by mixing 184 silicone elastomere base and 184 silicone elastomere curing with a 10:1 ratio. This mixture was used to fill completely the mould specifically designed for the SPR instrument. The silicone mixture was kept still for a period of 10 minutes at room temperature so bubbles could be removed from the mixture. The bubble-free moulds filled with silicone were than heated at 80°C for an hour. They were cooled to room temperature before the removal of the PDMS fluidic. The custom PDMS microfluidic generated was used to deliver the samples in the SPR/fluorescence instrument.

SPR-fluorescence instrumentation

The portable 4-channel SPR device used for biosensing has been previously described in the literature [46]. Herein, three channels were used as sensing channels, while the fourth channel served as a reference channel. Two types of SPR sensors were used in this study. The dove prisms were coated with a continuous gold film for a series of experiments. Microhole arrays were also mounted on a clean 20 x 12 x 3 mm glass dove prism with an RI-matching fluid. For both plasmonic materials, the custom made PDMS microfluidic was used to deliver the samples to the SPR sensor [46]. The fluidic was maintained in place with an aluminum arm latched to the main body of the instrument.

The fluorescence measurements were performed with a specifically designed fluorescence add-on fitted to the portable SPR device (Figure 1). A window was carved in the aluminum arm maintaining the fluidics in place (Figure 2). The excitation source was a laser diode at 532 nm (OZ-2000 series, OZ Optics, ltd., Ottawa, Canada). Fluorescence intensity was measured with an avalanche photodiode (APD130A, Thorlabs inc., Newton, NJ). Excitation and emission was filtered with a 532 nm dichroic beamsplitter and a 532 nm long-pass filter (Semrock, Inc., Rochester, NY). The fluorescence unit was 11 x 12 x 7 cm and latched to the top of the fluidic cell of the portable SPR device (Figure 1). The excitation and emission light were focused onto the surface of the SPR sensor and to the detector through a set of lenses. The fluorescence measurements were made through the PDMS of the fluidic cell. The fluorescence was read sequentially for each channel, which was then corrected with a reference measurement of fluorescence for a location outside of the fluidic channels. The signal was then additionally corrected with a background fluorescence measurement from PBS for all sensing channels. The fluorescence data reported were acquired from 3 scans of 10 data points/scan. The exposition time per data point was 0.1 s for Ampliflu[TM] Red.

Biosensor assembly

Monolayers of 3-mercaptopropionic acid-His-His-His-Asp-Asp-COOH (3-MPA-HHHDD-OH) were formed overnight on the gold surface of the SPR sensors with 1 mM solutions in dimethylformamide (DMF). The surface of the sensors were abundantly rinsed with ethanol to remove unbound molecules and dried with a stream of nitrogen. Specific biosensors for human PSA were constructed by using a protocol previously described elsewhere [47]. In brief, the monolayer was activated with ethyl-(dimethylaminopropyl)carbodiimide (EDC) and N-hydroxysuccinimide (NHS) coupling chemistry. Antibody solutions were prepared in phosphate buffer saline (PBS) at 75 µg/mL and incubated with the activated monolayer for covalent binding to the SPR sensor. PBS was then injected to remove all unbound antibodies. The unreacted NHS esters on the sensor surface were deactivated with a solution of 1 M ethanolamine hydrochloride adjusted to pH 8.5. PBS was injected once again to remove any remaining ethanolamine. The SPR biosensor was completed at this step and ready for detection of the target of interest.

PSA solutions were prepared in PBS 1x buffer at concentrations ranging from 0.1 pM to 1 µM. Biosensing of PSA was performed over 10 minutes in PBS with static flow incubation conditions. PSA was pre-incubated with a secondary antibody prior to injection into the SPR system. Mixing PSA with the anti-PSA in a total volume smaller than 20 µL for 10 minutes at room temperature formed a PSA/anti-PSA complex to increase sensitivity in SPR sensing. In the final step, dilution to a volume of 500µL was carried out using buffer.

PSA sensing with an SPR-ELISA assay

Please do not adjust margins
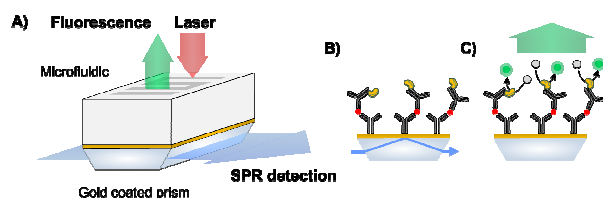**Lab on a Chip**
Page 4 of 8

Figure 3. A) Concept of the combination of SPR and fluorescence ELISA detection in a single microfluidic for the dual detection of the recognition event and enzymatic conversion. B) Schematic of the SPR biodetection and C) for the fluorescence measurement

Anti-PSA modified with horseradish peroxidase (HRP) was used for the fluorescent-ELISA assay. The ELISA assay was performed on the SPR sensor and detected in the SPR instrument using the fluorescence unit. In this fluorescent-ELISA assay, Ampliflu^{TM} Red peroxidase was incubated with an HRP-modified antibody to exhibit fluorescence with an excitation at a 532 nm. Anti-PSA labeled with HRP was pre-incubated with PSA for 10 minutes at room temperature using a molar ratio of 1:3 (PSA : anti-PSA). Thus, after the capture of PSA complex with anti-PSA labeled with HRP on the SPR sensor, the SPR sensor was incubated with 100 µM Ampliflu^{TM} Red solution prepared in PBS containing 20 mM H_2O_2. This assay led to fluorescence detection in the bulk solution due to the accumulation of the reaction product of HRP conversion of Ampliflu^{TM} Red contained in the SPR fluidics. Fluorescence was measured at intervals of 30, 90, 150, 300 and 600 s. The background signal in PBS was subtracted from the fluorescence.

Results and discussion

SPR-fluorescence instrument

The design of the SPR-fluorescence system was based on a 4-channel SPR instrument, which has been previously reported for monitoring methotrexate [46] and for monitoring a small therapeutic peptide directly in whole blood with a microdialysis chamber [48]. It was here modified to include fluorescence detection (see Figure SI1). The SPR instrument is powered by two USB cables from a laptop computer, has a small footprint and weight (1.8 kg), and has three sensing channels and a reference channel.

Several modifications to the SPR instrument were necessary to host the fluorescence unit. First, a window was carved into the aluminum arm that latches the fluidic cell in place (Figure 2). This window was aligned with the 4 channels of the SPR instrument to allow the upright fluorescence microscope to be mounted on the system. The fluorescence unit consisted of a laser entry port with a collimating lens directed to a long-pass dichroic beamsplitter matching the 532 nm laser excitation (Figure 1 and SI1). The laser was focused on a sensing channel using a lens. The emitted light was transmitted through the beamsplitter and a long-pass 532 nm filter, and was focused on an avalanche photodiode using another lens. The fluorescence unit was designed to analyze a single channel, thus it was mounted on railings and motorized

with a linear actuator to scan all 4 channels successively (Figure 1). The software was modified to include real-time fluorescence measurement in addition to the SPR sensorgrams (Figure SI2). A wavelength of 532 nm was selected for the current experiments due to the prevalence of fluorescence markers excited with this laser. However, the SPR-fluorescence instrument is not limited to this wavelength and other lasers, dichroic beamsplitters and filters can be used on the system according to the requirements of the analysis.

Microfluidics

Since both SPR and fluorescence analysis were performed in a single microfluidic device (Figure 3), the microfluidic cell used in this system required compatibility with SPR and fluorescence-ELISA. Beside providing a sealed environment for liquid handling, the microfluidic required a flat interface with the fluorescence unit to avoid background fluctuations from channel-to-channel, no defect or air bubbles and high transmission of fluorescent emission, which was fulfilled with molded PDMS. The fluidic cell was comprised of a sensing channel with an "S" shape to cover the three active sensors and a straight channel for the reference (Figure 2). The volume of the sensing channels of the microfluidic was also of importance. The channels of the fluidic cell must be about 1.5 mm wide to accommodate the SPR light beam. Smaller SPR light beams would lead to poorer signal-to-noise ratio of the SPR signal or longer integration times. The integration time per channel was set at 1 second with the 1 mm SPR beam, which was acceptable for providing detailed kinetic information in SPR. Longer integration times would lead to poorer time resolution of the measurements.

The fluorescence-ELISA was based on a peroxidase enzyme to generate a fluorescent product. Low microfluidic cell volumes would lead to low fluorescence due to limited the amount of available substrate that can be converted into its associated fluorophore. Large volumes would dilute the fluorescence of the product as the number of antibodies was set by the area of the SPR sensor and lead to poorer sensitivity or longer detection times. Thus, the fluidic channels were 800 µm deep for a total volume of 15 µL per channel. This microfluidic cell provided low background fluorescence and adequate fluidic handling for the SPR and fluorescence-ELISA experiments.

Microhole arrays

Many nano or microstructured plasmonic materials with different physical features have shown high sensitivity to refractive index change [49,50], which is an important feature improving detection limits in SPR sensing. Thus, highly sensitive microhole arrays with a periodicity of 3.2 microns and a hole diameter of 1.6 to 1.8 micron [51] were integrated to the SPR-fluorescence instrument. The original microhole array work was reported using a fabrication method that involved modified nanosphere lithography (NSL), and while this method of fabrication was suitable for the development of the microhole arrays, the technique has inhomogeneous coverage for microhole arrays on a large area of a few cm^2. This was
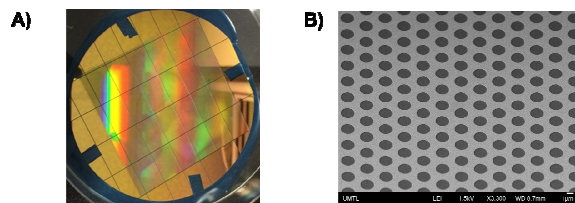
Figure 4. A) Photograph of microhole arrays produced by photolithography on a 4"
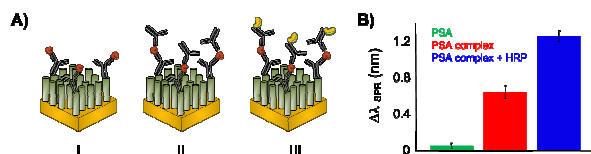wafer B) SEM image of the microhole arrays

Figure 5 A) Different biosensing schemes for PSA: direct detection (I), secondary
detection (II), anti-PSA labeled with HRP (III) B) SPR response for the detection of
10 nM PSA on microhole arrays for each biosensing scheme.

inadequate for the current SPR instrument due to the precise positioning of the sensing channels and the larger area covered by all 4 sensing channels in comparison to our previous SPR design [52]. Thus, the fabrication method of microhole arrays needed to be improved. A photolithographic process on a 4" glass wafer was developed to obtain a plasmonic crystalline structure on an area of nearly 100 cm^2. The wafer was diced into 24 homogeneous samples of 11 x 17 mm, which were then mounted on the dove prism SPR of 12 x 20 mm using RI-matching fluid. Photolithography led to a material with very few defects over a large surface (Figure 4).

The plasmonic properties of the microhole arrays fabricated by photolithography were assessed with the measurement of a binding event occurring on the SPR sensor and compared with a smooth and continuous Au film SPR sensor. The SPR response obtained for the immobilization of 500 nM anti-PSA on the SPR sensor increased from 2.22 ± 0.09 nm for the Au film to 5.19 ± 0.42 nm for the microhole arrays (Figure SI3). This SPR signal increase is around a factor of 2 to 3 with microhole arrays and is in agreement with a previous report using microhole arrays fabricated with nanosphere lithography [53].

Another interesting property of microhole arrays concerns the time required for the SPR response to reach equilibrium. All experiments with the SPR instrument were performed with static flow injection and anti-PSA was incubated with the SPR sensor and the binding followed in real-time. The association process of anti-PSA to the SPR surface was therefore diffusion limited. Microhole arrays have a smaller area of gold and thus fewer possible binding sites per unit area of the sensor in comparison to a smooth and continuous gold film. However, the SPR response at equilibrium was not only larger for microhole arrays, but the equilibrium was reached in a shorter time (Figure SI3). The time taken to reach 95% of the overall response was roughly 10 minutes for a continuous gold film and only 1.5 minutes for microhole arrays.

Enhanced fluorescence has been observed for fluorophores in close proximity to plasmonic substrates. Enhancement in fluorescence caused by the plasmonic material due to coupling effect requires close proximity of the fluorophore with the plasmonic material, in a region roughly defined as 20 to 50 nm from the gold film. Due to the instrumental configuration, the fluorescence signal collected here was generated by free fluorophores in solution and for the ones located in proximity to the plasmonic material. In the current assay, the

microfluidic channel is more than 100 microns high and thus, less than 1% of the molecules experienced enhanced fluorescence. Hence, enhanced fluorescence was not observed in this assay. Microhole arrays can enhance fluorescence and a proof-of-concept experiment was carried to show an approximately 5 to 10-fold enhancement in the fluorescence of anti-PSA labeled with a Zenon® fluorophore with the microhole arrays in comparison to the same assay performed on a gold film.

Surface plasmon resonance detection of PSA

The SPR instrument with the microhole arrays was validated with a biosensor for PSA, the current clinical biomarker for prostate cancer detection. PSA is a small protein (28 kDa) and thus detected with lower sensitivity in SPR sensing compared to larger proteins. The change in refractive index induced by the PSA protein binding to the sensor at 10 nM was near the detection limit while still at a relatively large concentration for PSA screening (Figure 5). Since the maximum level of PSA in serum considered normal for men over 50 years old is 0.15 nM [54,55], different configurations of the PSA bioassay with microhole arrays and SPR sensing were tested to meet these requirements. PSA was thus incubated with a secondary antibody to form a complex of larger mass (178 kDa) prior to injection into the SPR system. The increase in mass of the complex led to a larger change in the dielectric constant near the metallic film and thus a significant SPR response was observed (Figure 5). Detection of the PSA
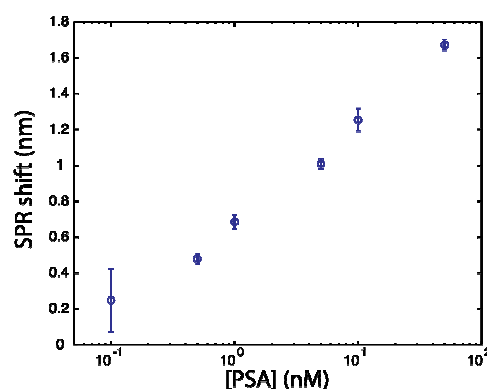

Figure 6. Calibration curve for PSA using the SPR assay. The detection was
performed with the PSA complex with anti-PSA modified with HRP. Error bars
represent one standard deviation for a triplicate measurement.

Please do not adjust margins
Lab on a Chip
Page 6 of 8

complex was possible using the secondary antibody enhancement at concentrations as low as 0.1 nM in PBS, which is the critical level of PSA for prostate cancer diagnostics.

In order to give a detectable fluorescence signal, the PSA complex was further modified. A fluorescence assay was adapted here for PSA detection by modifying the anti-PSA with a horseradish peroxidase (HRP) enzyme for the ELISA assay. The modifications performed on the PSA complex lead to a mass increase (222 kDa with HRP) and thus further amplified the SPR signal obtained for 10 nM PSA (Figure 5). A clear correlation was observed between the SPR signal and the mass of the PSA complex detected: 0.05 ± 0.03 nm for free PSA (28 kDa), 0.64 ± 0.07 nm with unlabeled anti-PSA (178 kDa) and 1.26 ± 0.06 nm with anti-PSA-HRP (222 kDa). The SPR sensor for PSA was then calibrated with antibodies modified with HRP. The SPR biosensor was able to detect PSA concentrations as low as 0.1 nM using the modified antibody assay (Figure 6). A negative control was also performed by incubating 10 nM human IgG with anti-PSA. The signal obtained for the negative control (-0.22 ± 0.13 nm) was negligible in comparison to 0.1 nM PSA (0.21 ± 0.03 nm).

Surface plasmon resonance-ELISA assay

An ELISA assay was created with the anti-PSA modified with HRP and Ampliflu[TM] Red. The ELISA assay was run directly on the SPR surface using microhole arrays and a thin Au film as previously outlined for PSA detection. This comparison of fluorescence detection on both surfaces was carried to verify whether the slightly smaller geometrical area of the microhole arrays (70% of the surface area of a thin Au film) had an impact on the fluorescence response of the ELISA assay for PSA. At a PSA concentration of 10 nM, the fluorescence response was nearly identical for both plasmonic sensor at 2743 ± 20 counts and 2855 ± 121 counts for the continuous gold film and the microhole arrays respectively. Thus, microhole arrays were used for both the SPR and fluorescence ELISA assays.

The optimization of experimental conditions was performed with the capture of 5 nM PSA complex modified with HRP. A solution containing Ampliflu[TM] Red and hydrogen peroxide was then injected into the SPR fluidic cell and fluorescence was monitored in real-time through the PDMS fluidic using the fluorescence unit mounted on the SPR instrument. Different concentrations of Ampliflu[TM]Red were injected to optimize the response gained from the ELISA. Fluorescence rapidly increased in the SPR fluidic cell to reach a maximum within approximately 5 minutes (Figure SI4). The ratio between Ampliflu[TM]Red and hydrogen peroxide (1:200) was always kept constant for this optimization. A slow decrease in signal was observed after an incubation of about 4 and 7.5 minutes for the most concentrated solutions of Ampliflu[TM]Red at 50 and 100 μM, respectively. This can most likely be explained by self-quenching of fluorescence due to the accumulation of the fluorescent compound in the SPR fluidic cell. Decreasing the concentration of Ampliflu[TM] Red injected from 100 to 10 μM improved the self-quenching issue, however this resulted in a smaller fluorescent signal in addition to a longer period of time required to reach the
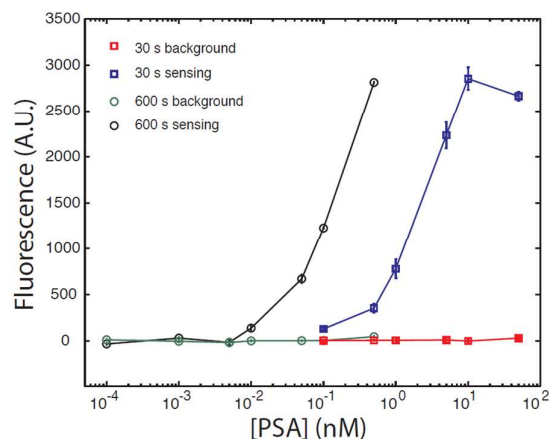

Figure 7. Calibration of the fluorescence output for PSA detection using the SPR-fluorescent ELISA assay. 100 μM of Ampliflu[TM] Red was incubated for 30 s and 600 s with HRP. The response from the sensing channel is shown in blue squares (30 s of reaction time) or black circles (600 s of reaction time) and the reference channel is shown in red squares (30 s of reaction time) or green circles (600 s of reaction time)

maximum observed signal. A 100 μM Ampliflu[TM] Red solution was thus chosen to obtain a large fluorescence signal over a short period of time.

A short incubation time of 30 seconds was sufficient to detect 0.1 nM PSA in the fluorescence assay using anti-PSA modified with HRP, a detection limit comparable to the SPR assays (Figure 7). The calibration revealed that the dynamic range was from 0.1 to 5 nM and this was performed using triplicate measurements. No response was measured from the reference channel (Data points in green and red, Figure 7) where a blank sample, which did not contain the PSA with anti-PSA-HRP complex, was injected. The calibration curve fish-hooked at higher concentrations of PSA and the fluorescence response at 50 nM PSA was smaller than for 10 nM PSA. This decrease in fluorescence was again very likely due to self-quenching of the fluorescent compound. Nevertheless, an underestimation of the amount of PSA in solution could arise if fluorescence was performed alone and so SPR detection could in this case provide a useful control to the fluorescence data, as SPR is still linear in this concentration range and does not fishhook at high concentrations.

The sensitivity of the fluorescence-ELISA assay can be improved with longer incubation times. Thus, the assay was lengthened to 10 minutes instead of 30 seconds. An order of magnitude in sensitivity was gained and detection limits of 10 pM were possible (Figure 7). Concentrations below 10 pM PSA were not statistically different from the results obtained for the reference channel and the limit of detection was established at 10 pM for the ELISA-based fluorescence assay.

The comparison of SPR and the fluorescence-ELISA for PSA revealed that both assays were sensitive for an overlapping dynamic range for short ELISA incubation times. ELISA was more sensitive if longer incubation times were used. The combination of SPR and fluorescence had significant advantages. Firstly, the dual detection of PSA with SPR and fluorescence provides an imbedded validation, which increases

the confidence of the results for concentrations where SPR and fluorescence are both linear (0.1 to 5 nM). This concentration range coincides with the clinically relevant range for patients suspected of developing prostate cancer (PSA levels above 150 pM). The second advantage concerns the extended dynamic range accessible using the SPR-ELISA assay. Using a single sample, set of reagents and set of experimental parameters, SPR coupled to a fluorescence-ELISA can quantify PSA concentrations ranging from 10 pM to nearly 50 nM. This dynamic range of the combined assay reached nearly 4 orders of magnitude far exceeding the dynamic range of a typical ELISA, which is in the region of 2 orders of magnitude.

Conclusions

The combination of SPR and fluorescence was achieved using a small and portable instrument proficient in the detection of PSA. Analysis of this prostate cancer biomarker by both SPR and fluorescence was achieved in a single microfluidic at concentration level relevant for diagnostic. SPR sensing provided real time analysis of biomolecule binding events whereas the use of microhole arrays as the plasmonic substrate allowed for the sensitive detection of PSA from 0.1 nM up to 50 nM within 2 minutes using a secondary antibody. The microhole arrays provided a 2-fold increase in SPR response. By introducing an HRP-modified secondary antibody into the assay, fluorescent detection was achieved using the modified SPR-fluorescence setup. This assay was more sensitive than SPR and had a dynamic range starting at 10 pM, which could be extended to 5 nM depending on the analysis time. The dynamic range of both techniques overlapped from 100 pM to 5 nM and so concentrations within this range will have an imbedded control. The dual SPR-fluorescence assay described herein was effective in the detection of PSA contained in a single sample at concentrations relevant for clinical diagnostics (10 pM to 50 nM) with an analysis time of 12 minutes. Thus, the extended range of PSA concentrations accessible to dual SPR-fluorescence detection covers that of healthy patients and the elevated concentrations of patients with prostate cancer. This setup could be extremely useful for the rapid staging of this disease, detecting PSA concentrations down to 0.1 nM.

Acknowledgements

References

(1)   Piliarik, M.; Homola, J. *Opt. Express* **2009**, *17*, 16505.

(2)   Tombelli, S.; Minunni, A.; Mascini, A. *Biosens. Bioelectron.* **2005**, *20*, 2424.

(3)   Win, M. N.; Klein, J. S.; Smolke, C. D. *Nucleic Acids Res.* **2006**, *34*, 5670.

(4)   Fagerstam, L. G.; Frostell, A.; Karlsson, R.; Kullman, M.; Larsson, A.; Malmqvist, M.; Butt, H. *Journal of molecular recognition : JMR* **1990**, *3*, 208.

(5)   Dunne, L.; Daly, S.; Baxter, A.; Haughey, S.; O'Kennedy, R. *Spectr. Lett.* **2005**, *38*, 229.

(6)   Dupont, D.; Muller-Renaud, S. *J. AOAC Int.* **2006**, *89*, 843.

(7)   Indyk, H. E.; Filonzi, E. L.; Gapper, L. W. *J. AOAC Int.* **2006**, *89*, 898.

(8)   Li, Y.; Lee, H. J.; Corn, R. M. *Anal. Chem.* **2007**, *79*, 1082.

(9)   Wittekindt, C.; Fleckenstein, B.; Wiesmuller, K. H.; Eing, B. R.; Kuhn, J. E. *J. Virol. Methods* **2000**, *87*, 133.

(10)   Eteshola, E.; Leckband, D. *Sensors and Actuators B-Chemical* **2001**, *72*, 129.

(11)   Christodoulides, N.; Mohanty, S.; Miller, C. S.; Langub, M. C.; Floriano, P. N.; Dharshan, P.; Ali, M. F.; Bernard, B.; Romanovicz, D.; Anslyn, E.; Fox, P. C.; McDevitt, J. T. *Lab on a Chip* **2005**, *5*, 261.

(12)   Dupuy, A. M.; Lehmann, S.; Cristol, J. P. *Clinical Chemistry and Laboratory Medicine* **2005**, *43*, 1291.

(13)   Goluch, E. D.; Nam, J.-M.; Georganopoulou, D. G.; Chiesl, T. N.; Shaikh, K. A.; Ryu, K. S.; Barron, A. E.; Mirkin, C. A.; Liu, C. *Lab on a Chip* **2006**, *6*, 1293.

(14)   Henares, T. G.; Mizutani, F.; Hisamoto, H. *Analytica Chimica Acta* **2008**, *611*, 17.

(15)   Lee, B. S.; Lee, J.-N.; Park, J.-M.; Lee, J.-G.; Kim, S.; Cho, Y.-K.; Ko, C. *Lab on a Chip* **2009**, *9*, 1548.

(16)   Ng, A. H. C.; Uddayasankar, U.; Wheeler, A. R. *Analytical and Bioanalytical Chemistry* **2010**, *397*, 991.

(17)   Chin, C. D.; Laksanasopin, T.; Cheung, Y. K.; Steinmiller, D.; Linder, V.; Parsa, H.; Wang, J.; Moore, H.; Rouse, R.; Umviligihozo, G.; Karita, E.; Mwambarangwe, L.; Braunstein, S. L.; van de Wijgert, J.; Sahabo, R.; Justman, J. E.; El-Sadr, W.; Sia, S. K. *Nature Medicine* **2011**, *17*, 1015.

(18)   Berg, B.; Cortazar, B.; Tseng, D.; Ozkan, H.; Feng, S.; Wei, Q.; Chan, R. Y.-L.; Burbano, J.; Farooqui, Q.; Lewinski, M.; Di Carlo, D.; Garner, O. B.; Ozcan, A. *ACS Nano* **2015**, *9*, 7857.

(19)   Rossier, J. S.; Girault, H. H. *Lab on a Chip* **2001**, *1*, 153.

(20)   Chon, H.; Lim, C.; Ha, S.-M.; Ahn, Y.; Lee, E. K.; Chang, S.-I.; Seong, G. H.; Choo, J. *Analytical Chemistry* **2010**, *82*, 5290.

(21)   Luo, Y.; Yu, F.; Zare, R. N. *Lab on a Chip* **2008**, *8*, 694.

(22)   de Melo, J. V.; Soldatkin, A. P.; Martelet, C.; Jaffrezic-Renault, N.; Cosnier, S. *Biosensors and Bioelectronics* **2003**, *18*, 345.

(23)   Soldatkin, A. P.; Montoriol, J.; Sant, W.; Martelet, C.; Jaffrezic-Renault, N. *Biosensors and Bioelectronics* **2003**, *19*, 131.

(24)   Yamazaki, T.; Kojima, K.; Sode, K. *Analytical Chemistry* **2000**, *72*, 4689.

(25)   Kolossov, V. L.; Spring, B. Q.; Clegg, R. M.; Henry, J. J.; Sokolowski, A.; Kenis, P. J. A.; Gaskins, H. R. *Experimental Biology and Medicine* **2011**, *236*, 681.

(26)   Kang, D.; Vallée-Bélisle, A.; Porchetta, A.; Plaxco, K. W.; Ricci, F. *Angewandte Chemie International Edition* **2012**, *51*, 6717.

(27)   Vallée-Bélisle, A.; Ricci, F.; Plaxco, K. W. *Journal of the American Chemical Society* **2012**, *134*, 2876.

(28)   Andersson, O.; Nikkinen, H.; Kanmert, D.; Enander, K. *Biosensors and Bioelectronics* **2009**, *24*, 2458.

(29)   Tawa, K.; Yokota, Y.; Kintaka, K.; Nishii, J.; Nakaoki, T. *Sensors and Actuators B: Chemical* **2011**, *157*, 703.

(30)   Inci, F.; Filippini, C.; Baday, M.; Ozen, M. O.; Calamak, S.; Durmus, N. G.; Wang, S.; Hanhauser, E.; Hobbs, K. S.; Juillard, F.; Kuang, P. P.; Vetter, M. L.; Carocci, M.; Yamamoto, H. S.; Takagi, Y.; Yildiz, U. H.; Akin, D.; Wesemann, D. R.; Singhal, A.; Yang, P. L.; Nibert, M. L.; Fichorova, R. N.; Lau, D. T.-Y.; Henrich, T. J.; Kaye, K. M.; Schachter, S. C.; Kuritzkes, D. R.; Steinmetz, L. M.; Gambhir, S. S.; Davis, R. W.; Demirci, U. *Proceedings of the National Academy of Sciences* **2015**, *112*, E4354.

(31)   Avramis, V. J.; Avramis, E. V.; Hunter, W.; Long, M. C. *Anticancer Research* **2009**, *29*, 299.

(32)   Campbell, K.; Huet, A.-C.; Charlier, C.; Higgins, C.; Delahaut, P.; Elliott, C. T. *Journal of Chromatography B-Analytical Technologies in the Biomedical and Life Sciences* **2009**, *877*, 4079.

(33)   Chung, J. W.; Kim, S. D.; Bernhardt, R.; Pyun, J. C. *Sensors and Actuators B-Chemical* **2005**, *111*, 416.

(34)   Lung, F. D. T.; Chen, H. Y.; Lin, H. T. *Protein and Peptide Letters* **2003**, *10*, 313.

(35)   Mahajan, S. S.; Iyer, S. S. *Journal of Carbohydrate Chemistry* **2012**, *31*, 447.

(36)   Nechansky, A. *Journal of Pharmaceutical and Biomedical Analysis* **2010**, *51*, 252.

(37)   Vaisocherova, H.; Faca, V. M.; Taylor, A. D.; Hanash, S.; Jiang, S. *Biosensors & Bioelectronics* **2009**, *24*, 2143.

(38)   Vashist, S. K.; Saraswat, M.; Holthoefer, H. *2nd International Conference on Bio-Sensing Technology* **2012**, *6*, 184.

(39)   Eggers, K. M.; Oldgren, J.; Nordenskjold, A.; Lindahl, B. *Am. Heart J.* **2004**, *148*, 574.

(40)   Dao, Q.; Krishnaswamy, P.; Kazanegra, R.; Harrison, A.; Amirnovin, R.; Lenert, L.; Clopton, P.; Alberto, J.; Hlavin, P.; Maisel, A. S. *J. Am. Coll. Cardiol.* **2001**, *37*, 379.

(41)   Yamamoto, M.; Baba, H.; Kakeji, Y.; Endo, K.; Ikeda, Y.; Toh, Y.; Kohnoe, S.; Okamura, T.; Maehara, Y. *Oncology* **2004**, *67*, 19.

(42)   Gann, P. H.; Hennekens, C. H.; Stampfer, M. J. *JAMA-J. Am. Med. Assoc.* **1995**, *273*, 289.

(43)   Kuriyama, M.; Wang, M. C.; Papsidero, L. D.; Killian, C. S.; Shimano, T.; Valenzuela, L.; Nishiura, T.; Murphy, G. P.; Chu, T. M. *Cancer Research* **1980**, *40*, 4658.

(44)   Besselink, G. A. J.; Kooyman, R. P. H.; van Os, P.; Engbers, G. H. M.; Schasfoort, R. B. M. *Anal. Biochem.* **2004**, *333*, 165.

(45)   Huang, L.; Reekmans, G.; Saerens, D.; Friedt, J. M.; Frederix, F.; Francis, L.; Muyldermans, S.; Campitelli, A.; Van Hoof, C. *Biosens. Bioelectron.* **2005**, *21*, 483.

(46)   Zhao, S. S.; Bukar, N.; Toulouse, J. L.; Pelechacz, D.; Robitaille, R.; Pelletier, J. N.; Masson, J. F. *Biosens. Bioelectron.* **2015**, *64*, 664.

(47)   Ratel, M.; Provencher-Girard, A.; Zhao, S. S.; Breault-Turcot, J.; Labrecque-Carbonneau, J.; Branca, M.; Pelletier, J. N.; Schmitzer, A. R.; Masson, J. F. *Anal. Chem.* **2013**, *85*, 5770.

(48)   Breault-Turcot, J.; Masson, J.-F. *Chemical Science* **2015**, *6*, 4247.

(49)   Shalabney, A.; Abdulhalim, I. *Laser Photon. Rev.* **2011**, *5*, 571.

(50)   Breault-Turcot, J.; Masson, J. F. *Anal. Bioanal. Chem.* **2012**, *403*, 1477.

(51)   Live, L. S.; Dhawan, A.; Gibson, K. F.; Poirier-Richard, H. P.; Graham, D.; Canva, M.; Vo-Dinh, T.; Masson, J. F. *Anal. Bioanal. Chem.* **2012**, *404*, 2859.

(52)   Bolduc, O. R.; Live, L. S.; Masson, J.-F. *Talanta* **2009**, *77*, 1680.

(53)   Live, L. S.; Dhawan, A.; Gibson, K. F.; Poirier-Richard, H.-P.; Graham, D.; Canva, M.; Vo-Dinh, T.; Masson, J.-F. *Analytical and Bioanalytical Chemistry* **2012**, *404*, 2859.

(54)   Makarov, D. V.; Trock, B. J.; Humphreys, E. B.; Mangold, L. A.; Walsh, P. C.; Epstein, J. I.; Partin, A. W. *Urology* **2007**, *69*, 1095.

(55)   Labrie, F.; Candas, B.; Dupont, A.; Cusan, L.; Gomez, J. L.; Suburu, R. E.; Diamond, P.; Levesque, J.; Belanger, A. *Prostate* **1999**, *38*, 83.

(56)   Poirier-Richard, H. P.; Couture, M.; Brule, T.; Masson, J. F. *Analyst* **2015**, *140*, 4792.

TOC graph